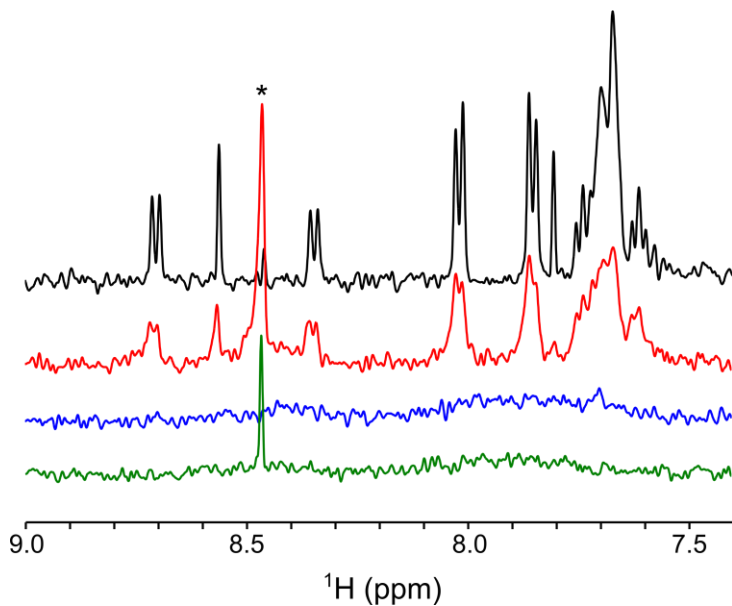


## Monomeric $\alpha$ -Synuclein Binds Congo Red Micelles in a Disordered Manner

Alexander S. Maltsev, Alexander Grishaev, and Ad Bax

Laboratory of Chemical Physics, National Institute of Diabetes and Digestive and Kidney  
Diseases, National Institutes of Health, Bethesda, Maryland 20892-0520

### **SUPPORTING INFORMATION**



**Figure S1.**  $^1\text{H}$  NMR spectra of Congo Red under different conditions: 0.5  $\mu\text{M}$  CR in 1:1 deuterated isopropanol:D2O at pH 6 (black); 2  $\mu\text{M}$  CR in 1:1 deuterated isopropanol:D2O at pH 6 (red); 0.5  $\mu\text{M}$  CR in D2O at pH 6 (blue), 0.5  $\mu\text{M}$  CR in D2O at pH 8.6 (green). Notice that already at 2  $\mu\text{M}$  in 1:1 isopropanol:D2O there is significant broadening of CR peaks indicative of aggregation. In the absence of isopropanol, CR is strongly aggregated already at 0.5  $\mu\text{M}$  concentration. Buffer pH has a strong effect on macroscopic behavior of CR solutions; in particular, there is higher propensity for precipitate formation at lower pH. However, we observed no narrow peaks in  $^1\text{H}$  NMR spectra of 0.5  $\mu\text{M}$  CR at pH values as high as 8.6 in the absence of isopropanol.

Experiments were collected on a 500 MHz spectrometer equipped with a cryo-probe at 30 °C. For 0.5  $\mu\text{M}$  samples 16,000 scans were collected, and for the 2  $\mu\text{M}$  sample 1000 scans were collected, so as to match the signal to noise ratios. The spectrum of the 2  $\mu\text{M}$  sample was scaled up 4-fold, to match the signal levels. The asterisk marks a likely impurity.

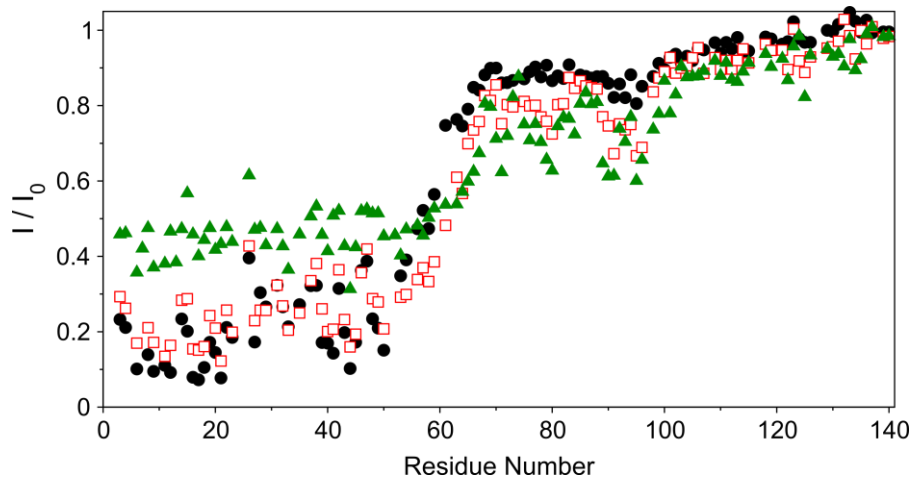


**Figure S2.** Effect of sample concentration on intensity attenuation ( $I/I_0$ ) in the presence of Congo Red (15 °C, pH 6.0,  $^2\text{H}/^{15}\text{N}$ -aS, 500 MHz). A 200  $\mu\text{M}$  sample with equimolar concentrations of aS and CR was prepared, and was subsequently diluted to different concentrations. Shown are relative intensities of HSQC peaks compared to free protein for the following samples: 50  $\mu\text{M}$  aS (black filled circles), 6  $\mu\text{M}$  aS (red open squares), 2  $\mu\text{M}$  aS (green filled triangles).

Acquisition time was 180 ms in the  $^1\text{H}$  dimension and 165 ms in the  $^{15}\text{N}$  dimension. Spectra were apodized with a 72°-shifted sine bell window function in  $^1\text{H}$ , and with a cosine bell window function in the  $^{15}\text{N}$  dimension.

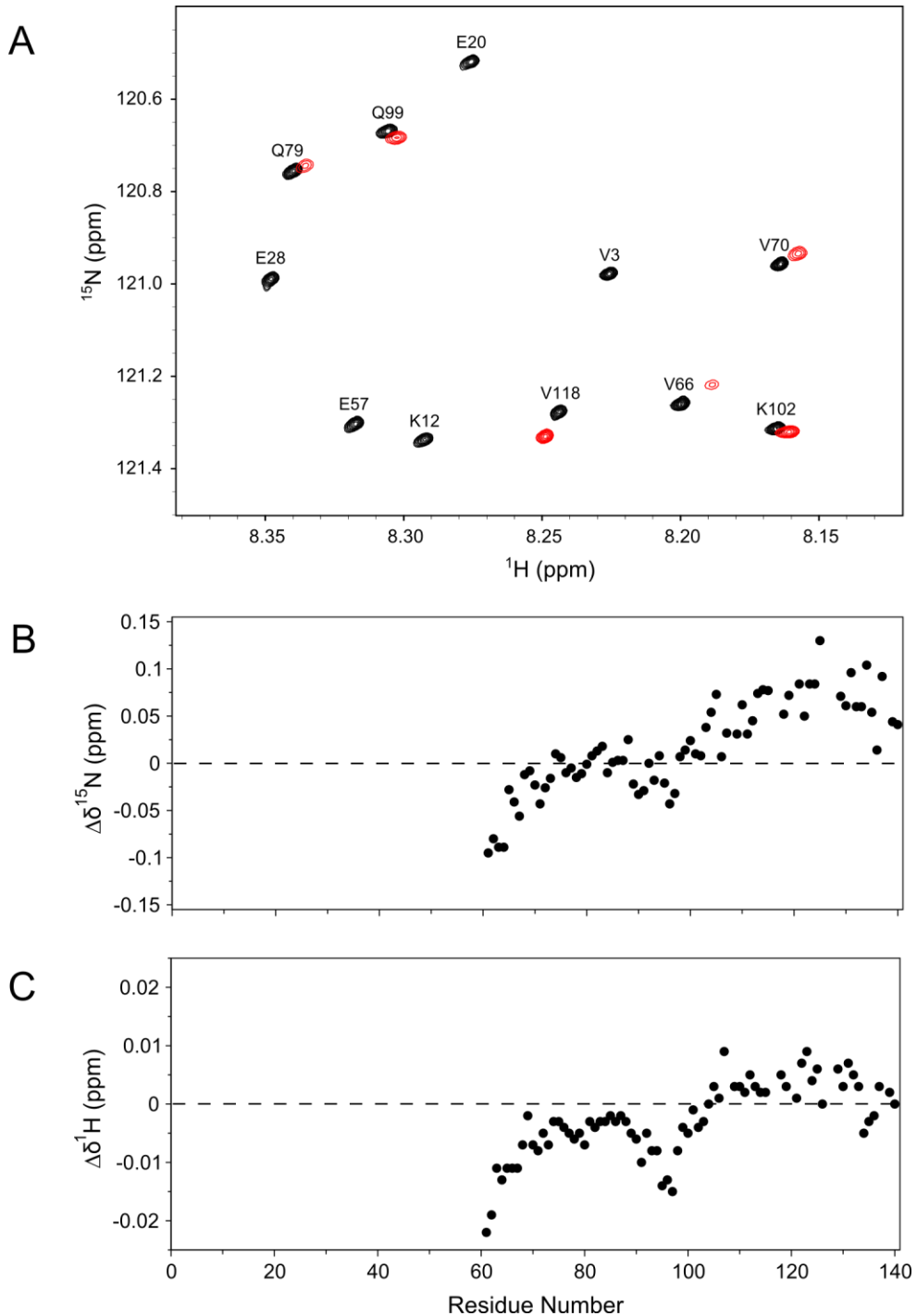


**Figure S3.** Backbone  $^{15}\text{N}$  and  $^1\text{H}^{\text{N}}$  chemical shift changes induced by Congo Red. (A) Overlay of expanded small regions of  $^{15}\text{N}$ - $^1\text{H}$  TROSY-HSQC spectra acquired for free aS (black) and at 4:1 CR:aS (red). Spectra were recorded on an 800 MHz spectrometer equipped with a cryo-probe at 15 °C on perdeuterated aS. Acquisition time in each dimension was 750 ms. Spectra were apodized with a 45°-shifted sine bell window function in both dimensions. (B)  $^{15}\text{N}$  chemical shift difference and (C)  $^1\text{H}^{\text{N}}$  chemical shift difference compared to free aS. The dashed horizontal lines indicate zero change.

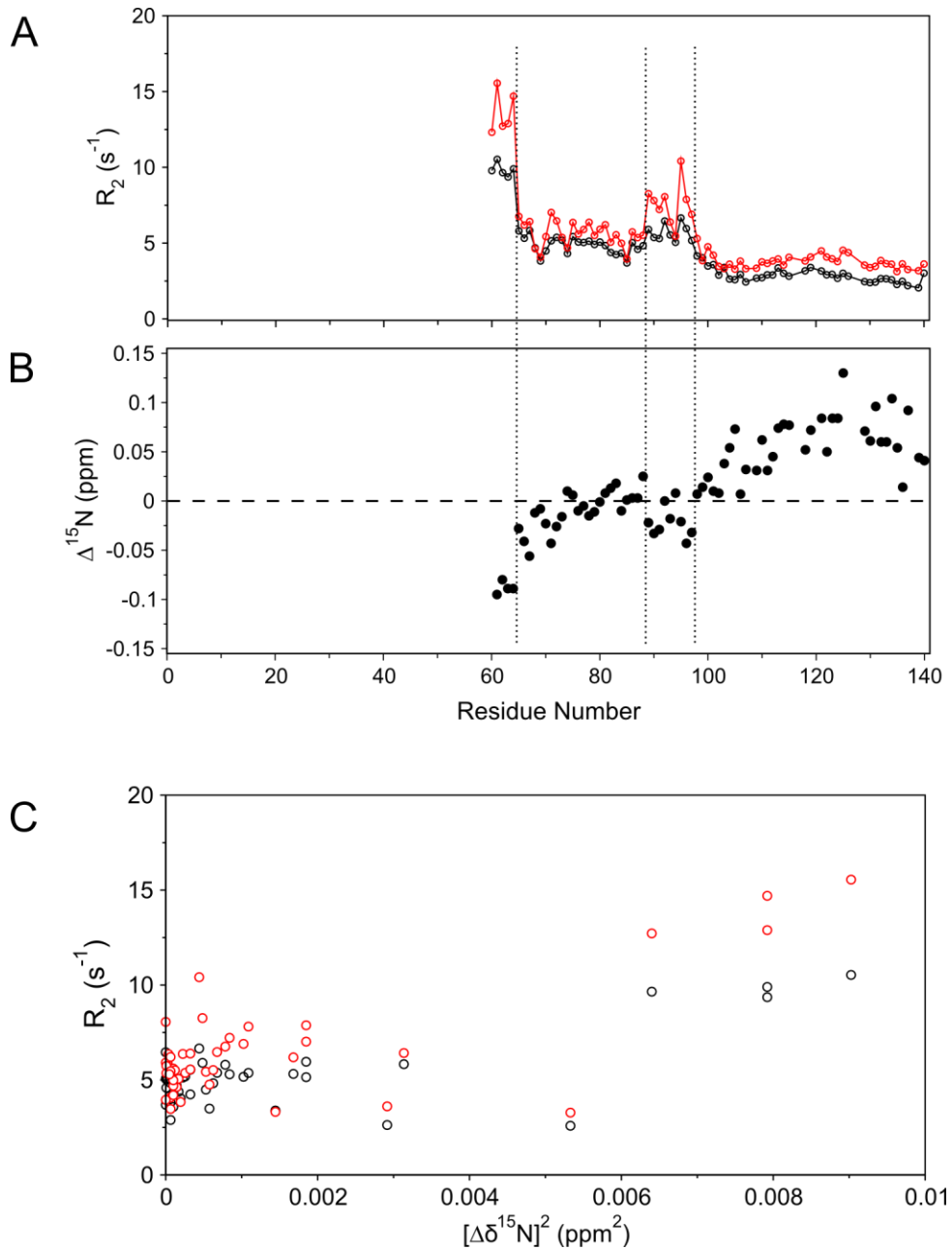


**Figure S4.** Results of CPMG  $R_2$  relaxation experiments performed on a sample with CR:aS of 4:1. (A) Relaxation rate measured for an effective field of 80 Hz at 500 MHz (black) and 800 MHz (red) as a function of residue number. (B) Change in  $^{15}\text{N}$  chemical shift compared to free protein. The dashed horizontal line in B provides the baseline for absence of chemical shift change. The dotted vertical lines serve to delineate regions with distinct behaviors. (C) Correlation of  $^{15}\text{N}$  squared chemical shift change with relaxation rate observed at 500 MHz (black) and 800 MHz (red) for residues 61-105.

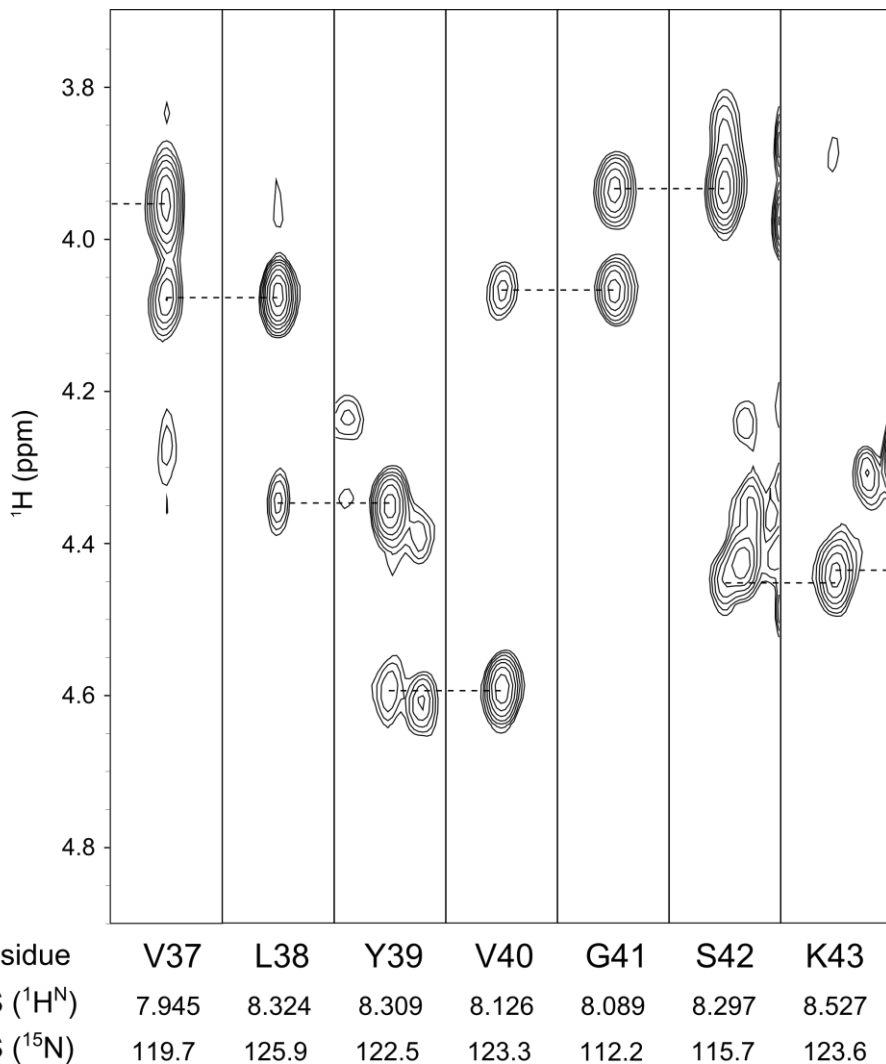


**Figure S5.** Strip plot of several sequential residues taken from the 600 MHz 3D HHN NOESY-HMQC spectrum of a sample with 1:1 molar ratio of CR:aS. In each strip the stronger peak corresponds to NOE from <sup>1</sup>H<sup>a</sup> of the preceding residue, and the weaker peak is the intraresidue <sup>1</sup>H<sup>a</sup>-<sup>1</sup>H<sup>N</sup> NOE. Notice the absence of d<sub>αN</sub>(i, i+3) NOE cross peaks, which would be characteristic of α-helix.

Spectra were recorded for fully protonated and <sup>15</sup>N-labeled aS, 200 μM, 15°C, pH 6.0. The NOE mixing time was 70 ms. Acquisition times were 54 ms in the <sup>15</sup>N dimension and 26 ms in the indirect <sup>1</sup>H dimension.

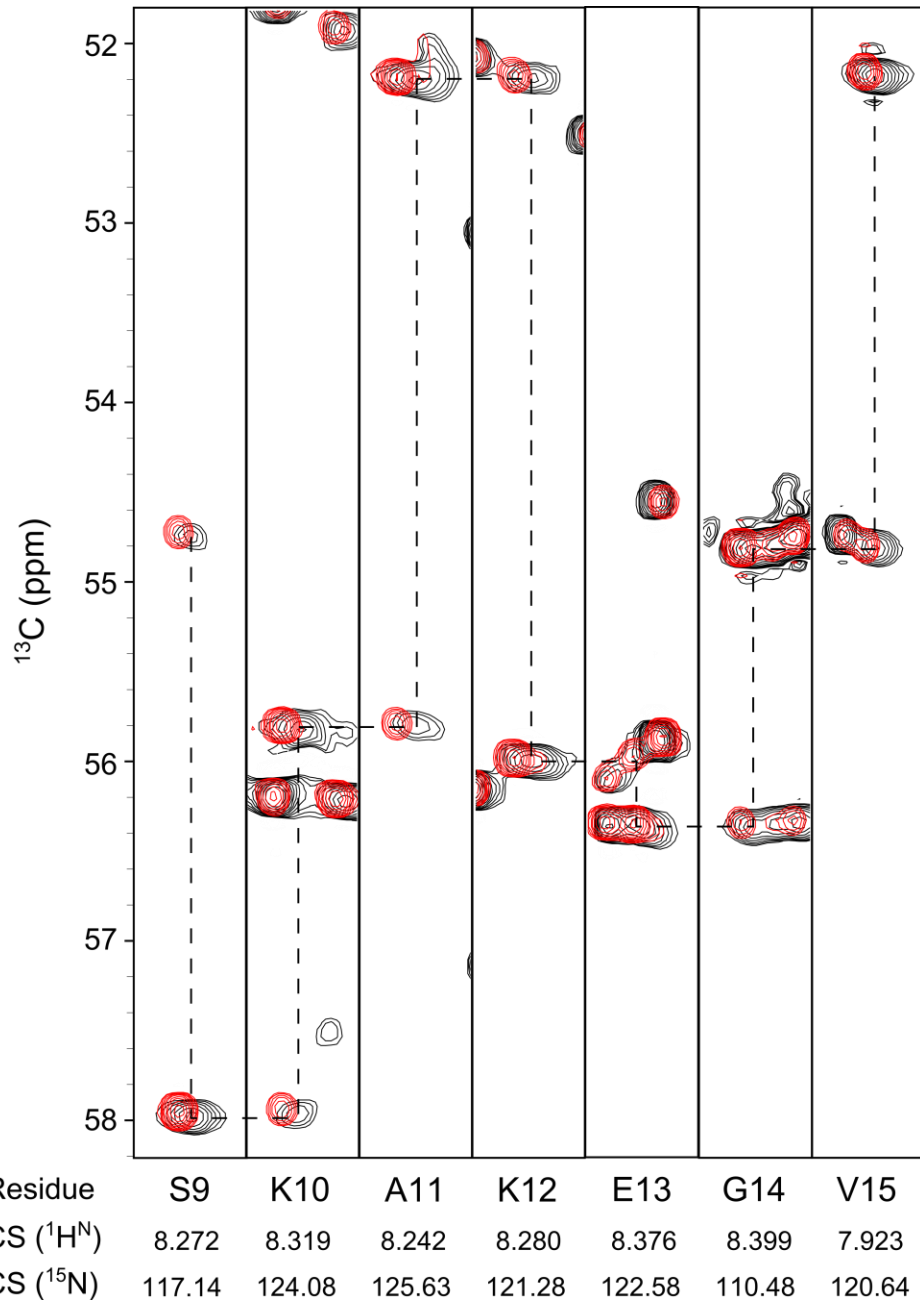


**Figure S6.** Superimposed strips taken from 3D CT-HNCA spectra of free aS (red), and of aS in the presence of Congo Red at 1:1 molar ratio (black). The spectra were collected on perdeuterated, <sup>15</sup>N- and <sup>13</sup>C-labeled aS, at 15°C, 200 μM, pH 6.0, on a 500 MHz spectrometer equipped with a cryo-probe. The spectra were folded in the <sup>13</sup>C dimension with the carrier at 56 ppm and a spectral width of 10 ppm. Constant-time evolution was used in the <sup>13</sup>C dimension with a total acquisition time of 26 ms. Mixed-time evolution (Ying et al, J. Biomol. NMR, 37, 195-204, 2007) was used in the <sup>15</sup>N dimension with an acquisition time of 100 ms.

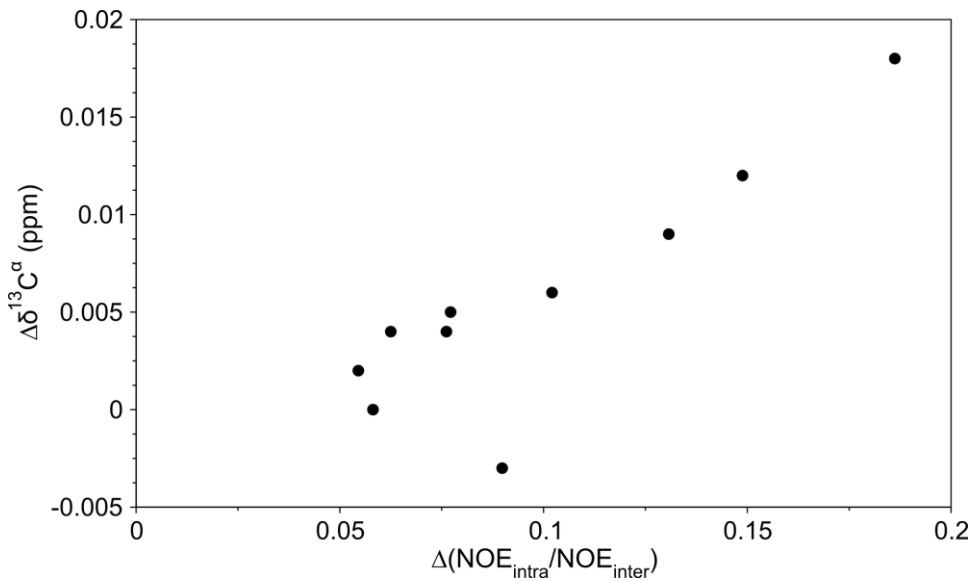


**Figure S7.** Plot of the change in the  $^{13}\text{C}^\alpha$  chemical shift of residue i versus the change in the intra- to inter-residue  $\text{H}^\alpha\text{-H}^N$  NOE ratio of residue i+1  $d_{\alpha\text{N}}(i+1,i+1)/d_{\alpha\text{N}}(i,i+1)$ . Data are shown where available for the first 50 residues of aS. Data points that had a Gly as residue i or i+1 are not included. Comparison is between free aS and 200  $\mu\text{M}$  1:1 CR:aS samples.

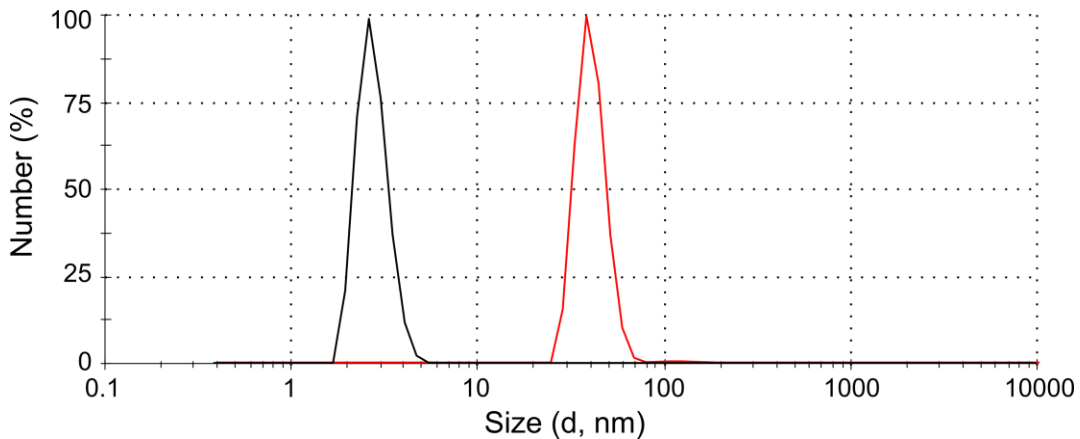


**Figure S8.** Particle diameter, d, as obtained from dynamic light scattering experiments performed on samples of 200  $\mu\text{M}$  alpha-synuclein + 200  $\mu\text{M}$  Congo Red in 20 mM sodium phosphate buffer at pH 6 (red trace), and in 100 mM Tris buffer at pH 7.4 (black trace). The figure shows DLS data weighted by the number of particles. Measurements were performed on a Malvern Zetasizer Nano instrument (using a 532 nm laser) at 15°C.

Table S1. Attenuation of TROSY-HSQC  $^1\text{H}$ - $^{15}\text{N}$  correlation intensities,  $I/I_0$ , as a function of CR:aS molar ratio. Four ratios are presented: 1:4, 1:2, 2:1, 8:1. Data used for generating Figure 1B, main text.

Residue	1:4 CR:aS	1:2 CR:aS	2:1 CR:aS	8:1 CR:aS
3	0.705	0.374	—	—
4	0.663	0.335	—	—
6	0.628	0.247	—	—
7	0.633	—	—	—
8	0.667	0.284	—	—
9	0.643	0.241	—	—
11	0.697	0.231	—	—
12	0.720	0.241	—	—
13	0.789	—	—	—
14	0.762	0.393	—	—
15	0.811	0.407	—	—
16	0.805	0.278	—	—
17	0.780	0.246	—	—
18	0.791	0.309	—	—
19	0.830	0.391	—	—
20	0.807	0.377	—	—
21	0.805	0.293	—	—
22	0.806	0.439	—	—
23	0.804	0.403	—	—
26	0.883	0.608	0.130	—
27	0.847	0.423	—	—
28	0.871	0.549	—	—
29	0.848	0.472	0.083	—
31	0.828	0.536	0.103	—
32	0.834	0.520	0.096	—
33	0.819	0.466	0.060	—
35	0.873	0.514	—	—
36	0.856	0.627	—	—
37	0.866	0.551	0.095	—
38	0.835	0.526	0.087	—
39	0.819	0.397	—	—
40	0.834	0.407	—	—
41	0.789	0.347	—	—
42	0.778	0.491	0.107	—
43	0.784	0.421	—	—
44	0.802	0.348	—	—

Table S1 (continued)

Residue	1:4 CR:aS	1:2 CR:aS	2:1 CR:aS	8:1 CR:aS
45	0.806	0.421	—	—
46	0.851	0.582	—	—
47	0.861	0.593	—	—
48	0.875	0.520	0.074	—
49	0.899	0.558	0.115	—
52	0.894	—	—	—
53	0.884	0.615	0.128	—
54	0.879	0.639	0.161	—
56	0.903	0.700	0.234	—
57	0.920	0.736	0.273	—
58	0.903	0.710	0.241	—
59	0.888	0.744	0.314	—
61	0.954	0.911	0.508	—
63	0.960	0.865	0.614	—
64	0.910	0.828	0.551	0.120
65	0.887	0.812	0.592	0.215
66	0.941	0.879	0.704	0.297
67	0.930	0.877	0.692	0.315
68	0.936	0.896	0.761	0.413
69	0.940	0.907	0.812	—
70	0.945	0.908	0.782	0.406
71	0.937	0.895	0.742	0.302
72	0.921	0.878	0.721	0.330
73	0.899	0.862	0.731	0.368
74	0.967	—	—	—
75	0.919	0.873	0.711	0.327
76	0.937	0.892	0.766	0.351
77	0.955	0.911	0.775	0.319
78	0.933	0.896	0.788	0.305
79	0.935	0.902	0.784	0.316
80	0.920	0.878	0.726	0.254
81	0.917	0.875	0.733	0.321
82	0.940	0.890	0.770	—
83	0.960	0.925	0.822	0.420
84	0.930	0.895	0.776	0.365
85	0.939	0.902	0.803	0.410

Table S1 (continued)

Residue	1:4 CR:aS	1:2 CR:aS	2:1 CR:aS	8:1 CR:aS
86	0.918	0.878	0.741	0.382
87	0.904	0.866	0.744	0.380
88	0.952	0.915	0.828	0.366
89	0.952	0.902	0.778	0.252
90	0.942	0.891	0.752	0.235
91	0.926	0.872	0.695	0.163
92	0.931	0.872	0.693	0.195
93	0.917	0.859	0.660	0.206
94	0.961	0.910	0.739	—
95	0.937	0.880	0.659	0.144
96	0.943	0.886	0.737	0.202
98	0.952	0.926	0.832	0.413
99	0.938	0.910	0.819	0.505
100	0.946	0.917	0.844	—
101	0.967	0.944	0.920	0.668
102	0.967	0.952	0.919	0.635
103	0.940	0.920	0.861	0.642
104	0.959	0.944	0.911	0.758
105	0.956	0.946	0.911	0.723
106	0.971	0.952	0.975	0.862
107	0.950	0.943	0.878	0.704
109	0.957	0.940	0.948	0.829
110	0.962	0.958	0.825	0.778
111	0.965	0.952	0.964	0.850
112	0.961	0.946	0.897	0.772
113	0.947	0.924	0.911	0.791
114	0.956	0.934	0.892	0.746
115	0.956	0.936	0.899	0.848
118	0.963	0.937	0.935	0.816
119	0.961	0.951	0.919	0.805
121	0.960	0.939	0.911	0.835
122	0.962	0.970	0.880	0.845
123	0.987	0.995	0.928	—
124	0.965	0.969	0.958	0.914
125	0.978	0.951	0.867	0.865
126	0.974	0.969	0.884	—

Table S1 (continued)

Residue	1:4 CR:aS	1:2 CR:aS	2:1 CR:aS	8:1 CR:aS
129	0.981	0.981	0.929	0.903
130	0.981	0.964	0.967	0.907
131	—	—	0.971	0.949
133	1.001	1.002	0.967	—
134	0.984	0.979	0.980	1.003
135	0.979	0.997	0.993	0.980
136	0.989	0.987	1.003	0.979
137	0.994	0.967	0.959	0.955
139	0.995	0.990	1.000	0.968
140	0.983	0.966	0.966	0.930

Table S2. Chemical shift changes and peak intensity attenuation,  $I/I_0$ , for CR:aS of 0.8:1 compared to free aS. Data used for generating Figure 2, main text.

Residue	Delta N	Delta H	$I/I_0$	Residue	Delta N	Delta H	$I/I_0$
3	-0.013	-0.003	0.10	44	-0.024	-0.003	0.11
4	-0.016	-0.003	0.10	45	-0.013	-0.003	0.17
6	-0.024	-0.005	0.07	46	-0.010	-0.002	0.27
7	-0.013	-0.003	0.10	47	-0.007	-0.002	0.28
8	-0.007	-0.004	0.10	48	-0.002	-0.003	0.24
9	-0.026	-0.004	0.07	49	-0.013	-0.002	0.21
11	-0.026	-0.005	0.05	50	-0.003	-0.005	0.21
12	-0.023	-0.006	0.06	51	-0.020	-0.004	0.22
13	-0.015	-0.001	0.07	53	-0.013	-0.002	0.28
14	-0.015	-0.003	0.14	54	-0.008	-0.002	0.35
16	-0.027	-0.003	0.07	55	-0.012	-0.002	0.23
17	-0.026	-0.002	0.08	56	-0.008	-0.001	0.41
18	-0.021	-0.003	0.09	57	-0.007	-0.001	0.45
19	-0.016	-0.003	0.13	58	-0.007	-0.002	0.44
20	-0.021	-0.003	0.12	59	-0.005	-0.001	0.53
21	-0.023	-0.004	0.08	60	-0.008	-0.001	0.58
22	-0.012	-0.003	0.18	61	-0.002	0.000	0.61
23	-0.016	-0.003	0.15	62	-0.002	-0.001	0.64
24	-0.032	-0.004	0.12	63	-0.002	-0.001	0.67
25	-0.016	-0.003	0.18	64	-0.002	-0.001	0.67
26	0.001	-0.002	0.32	65	0.000	0.000	0.79
27	-0.021	-0.003	0.15	66	-0.002	-0.001	0.86
28	-0.017	-0.002	0.21	67	-0.002	-0.001	0.87
29	-0.018	-0.003	0.17	68	0.000	0.000	0.93
30	-0.007	-0.002	0.44	69	0.000	0.000	0.92
31	-0.008	-0.002	0.28	70	-0.001	0.000	0.91
32	-0.007	-0.002	0.25	71	-0.002	0.000	0.77
33	-0.017	-0.002	0.18	72	-0.001	0.000	0.75
35	-0.017	-0.002	0.19	73	0.000	0.000	0.82
36	-0.006	-0.002	0.30	74	0.001	0.000	0.85
37	-0.007	-0.002	0.24	75	0.001	0.000	0.90
38	-0.014	-0.002	0.22	76	0.000	0.000	0.89
39	-0.017	-0.003	0.13	77	0.000	0.000	0.89
40	-0.022	-0.002	0.12	78	0.000	0.000	0.77
41	-0.009	-0.003	0.16	79	0.000	0.000	0.88
42	-0.006	-0.002	0.32	80	0.000	0.000	0.84
43	-0.011	-0.003	0.21	81	0.001	0.000	0.86

Table S2 (continued)

Residue	Delta N	Delta H	I/I <sub>0</sub>	Residue	Delta N	Delta H	I/I <sub>0</sub>
82	0.000	0.000	0.88	123	0.011	0.001	0.94
83	0.002	0.000	0.91	124	0.011	0.000	0.96
84	0.000	0.000	0.91	125	0.017	0.001	0.90
85	0.000	0.000	0.96	126	0.020	0.001	0.87
86	0.000	0.000	0.86	129	0.010	0.001	0.90
87	0.000	0.000	0.89	130	0.010	0.001	0.88
88	0.001	0.000	0.89	131	0.013	0.001	0.88
89	0.000	0.000	0.74	132	0.005	0.001	0.90
90	0.000	0.000	0.86	133	0.005	0.001	0.90
91	0.000	0.000	0.82	134	0.010	-0.001	0.87
92	0.001	0.000	0.81	135	0.010	0.000	1.01
93	0.000	0.000	0.86	136	-0.005	-0.001	0.87
94	0.001	0.000	0.85	137	0.012	0.002	0.91
95	0.000	-0.001	0.88	139	0.007	0.001	0.98
96	-0.001	-0.001	0.82	140	0.000	0.000	1.02
97	-0.001	0.000	0.91				
98	0.002	0.000	0.92				
99	0.001	0.000	0.92				
100	0.002	0.000	0.89				
101	0.001	0.000	0.92				
102	0.000	0.000	0.87				
103	0.003	0.000	0.96				
104	0.004	0.000	0.93				
105	0.005	0.000	0.88				
106	0.001	0.000	0.99				
107	0.002	0.000	0.93				
109	0.003	0.000	0.95				
110	0.006	0.000	0.90				
111	0.002	0.000	0.93				
112	0.004	0.000	0.91				
113	0.009	0.000	0.96				
114	0.010	0.001	1.00				
115	0.008	0.000	0.92				
118	0.004	0.000	0.92				
119	0.009	0.000	0.92				
121	0.012	0.000	0.95				
122	0.003	0.001	0.88				

Table S3A. Attenuation of TROSY-HSQC  $^1\text{H}$ - $^{15}\text{N}$  correlation intensities,  $I/I_0$ , as a function of residue number for CR:aS = 0.8:1, for three different ionic strength conditions. Data used for Figure 3A, main text.

Residue	0 mM	100 mM	200 mM	Residue	0 mM	100 mM	200 mM
3	0.345	0.593	0.794	47	0.647	0.698	0.888
4	0.376	0.638	0.716	48	0.496	0.737	0.912
5	0.278	0.557	0.805	49	0.603	—	0.856
6	0.227	0.512	0.777	50	0.382	0.624	0.824
8	0.289	0.574	0.857	52	0.521	0.710	0.889
9	0.248	0.524	0.770	53	0.568	0.757	0.875
11	0.256	0.492	0.768	54	0.668	0.765	0.900
12	0.238	0.549	0.815	56	0.659	0.784	0.884
14	0.414	0.685	0.826	57	0.677	0.811	0.854
15	0.344	0.756	0.882	58	0.681	0.825	0.900
16	0.260	0.577	0.820	59	0.694	0.802	0.879
17	0.234	0.564	0.835	61	0.881	—	—
18	0.284	0.620	0.863	63	0.800	0.859	0.923
19	0.368	0.660	0.837	64	0.779	0.843	0.909
20	0.311	0.664	0.823	65	0.799	0.894	0.917
21	0.248	0.587	0.843	66	0.853	0.868	0.956
22	0.406	0.671	0.855	67	0.833	0.856	0.903
23	0.391	0.642	0.827	68	0.889	0.935	0.958
26	0.584	—	—	69	0.878	0.927	0.937
27	0.366	0.631	0.849	70	0.884	0.921	0.910
28	0.486	0.713	0.829	71	0.845	0.870	0.912
29	0.468	0.714	0.860	72	0.850	0.889	0.920
31	0.530	0.696	0.880	73	0.855	0.888	0.944
32	0.485	0.717	0.875	74	0.869	0.911	0.926
33	0.429	0.689	0.893	75	0.844	0.904	0.941
35	0.451	0.761	0.834	76	0.861	0.856	0.918
36	0.547	0.784	0.941	77	0.862	0.891	0.905
37	0.530	0.740	0.922	78	0.892	0.915	0.940
38	0.487	0.689	0.880	79	0.865	0.950	0.910
39	0.362	0.652	0.869	80	0.836	0.906	0.920
40	0.363	0.638	0.875	81	0.851	0.887	0.926
41	0.344	0.636	0.867	82	0.837	0.929	0.906
42	0.509	0.750	0.838	83	0.859	0.901	0.887
43	0.424	0.631	0.813	84	0.857	0.916	0.946
44	0.301	0.606	0.828	85	0.893	0.934	0.954
45	0.354	0.540	0.896	86	0.876	0.919	0.948
46	0.529	0.766	0.897	87	0.895	0.924	0.956

Table S3A (continued)

Residue	0 mM	100 mM	200 mM	Residue	0 mM	100 mM	200 mM
88	0.894	0.923	0.944	126	0.958	0.982	0.959
89	0.848	0.880	0.929	129	0.932	0.961	0.960
90	0.875	0.921	0.954	130	0.943	0.988	0.924
91	0.835	0.846	0.942	132	1.034	—	0.895
92	0.859	0.876	0.924	133	1.026	1.031	0.984
93	0.846	0.916	0.914	134	0.975	0.981	1.022
94	0.865	0.904	0.930	135	0.962	1.000	0.982
95	0.853	0.897	0.918	136	0.973	—	0.990
96	0.850	0.879	0.910	137	0.945	1.014	0.986
98	0.881	0.939	0.925	139	0.943	0.966	0.948
99	0.885	0.921	0.922	140	0.972	0.986	1.027
100	0.886	0.895	0.914				
101	0.894	0.961	0.928				
102	0.924	0.921	0.966				
103	0.874	0.925	0.928				
104	0.879	0.964	0.919				
105	0.908	—	1.027				
106	0.921	0.953	0.976				
107	0.916	0.971	0.957				
109	0.886	0.929	0.952				
110	0.893	0.954	0.926				
111	0.885	0.963	0.948				
112	0.913	0.983	1.020				
113	0.919	0.966	0.920				
114	0.918	—	1.029				
115	0.903	0.925	0.927				
116	0.899	0.953	1.004				
118	0.923	0.974	0.960				
119	0.919	0.970	0.920				
121	0.948	0.966	0.980				
122	0.988	0.983	0.991				
123	0.931	0.983	0.971				
124	0.989	0.966	0.989				
125	0.923	—	0.929				

Table S3B. Attenuation of TROSY-HSQC  $^1\text{H}$ - $^{15}\text{N}$  correlation intensities,  $I/I_0$ , as a function of residue number for CR:aS = 4:1, for three different ionic strength conditions. Data used for Figure 3B, main text.

Residue	0 mM	100 mM	200 mM	Residue	0 mM	100 mM	200 mM
59	0.112	—	—	96	0.381	0.174	0.171
60	0.092	0.044	0.036	97	—	0.181	0.141
61	0.147	0.111	0.115	98	0.607	0.429	0.262
62	0.111	0.119	0.184	99	0.669	0.528	0.330
63	0.180	0.145	0.171	100	0.657	0.445	0.398
64	0.194	0.128	0.151	101	0.746	0.630	0.410
65	0.349	0.308	0.219	102	0.755	0.611	0.394
66	0.400	0.355	0.320	103	0.794	0.732	0.431
67	0.496	0.400	0.354	104	0.799	0.796	0.447
68	0.603	0.582	0.426	105	0.820	0.726	0.551
69	0.626	0.579	0.409	106	0.845	0.808	0.582
70	0.565	0.491	0.391	107	0.790	0.830	0.487
71	0.462	0.360	0.305	109	0.849	0.901	0.593
72	0.532	0.408	0.368	110	0.836	0.878	0.596
73	0.579	0.508	0.397	111	0.847	0.895	0.625
74	0.612	0.539	0.415	112	0.817	0.877	0.727
75	0.537	0.376	0.328	113	0.860	0.868	0.631
76	0.568	0.406	0.367	114	—	—	0.715
77	0.526	0.339	0.304	115	0.829	0.884	0.666
78	0.510	0.394	0.376	116	0.812	0.860	0.682
79	0.528	0.406	0.325	118	0.882	0.919	0.662
80	0.483	0.364	0.277	119	0.904	0.894	0.688
81	0.536	0.386	0.318	121	0.931	0.957	0.916
82	0.544	0.402	0.292	122	0.944	0.952	0.930
83	0.591	0.449	0.394	123	0.996	0.988	1.022
84	0.585	0.477	0.364	124	0.999	0.963	0.954
85	0.641	0.523	0.423	125	0.955	—	—
86	0.594	0.495	0.444	126	0.999	0.919	0.906
87	0.621	0.492	0.346	129	0.940	0.922	0.960
88	0.553	0.456	0.347	130	0.959	0.986	0.957
89	0.442	0.254	0.247	131	—	—	0.957
90	0.432	0.245	0.247	134	1.010	0.942	1.004
91	0.353	0.186	0.199	135	1.038	0.958	0.990
92	0.391	0.203	0.188	136	0.976	1.098	0.905
93	0.443	0.295	0.213	137	0.952	0.977	0.937
94	—	0.373	0.203	139	0.944	0.941	0.972
95	0.289	0.141	0.144	140	0.929	0.946	1.029

Table S4. Relaxation rates measured at 80 Hz CPMG effective field at 500 MHz and 900 MHz as well as squared <sup>15</sup>N chemical shift changes relative to free aS. Sample conditions are: 15 °C, pH 6.0, 200 μM aS, 260 μM CR. Data used for generating Figure 4, main text.

Residue	$[\Delta\delta N]^2$ , ppm <sup>2</sup>	R2, Hz 500 MHz	R2, Hz 900 MHz	Residue	$[\Delta\delta N]^2$ , ppm <sup>2</sup>	R2, Hz 500 MHz	R2, Hz 900 MHz
3	0.0036	6.5	10.7	35	0.0059	7.4	14.0
4	0.0040	8.6	16.1	36	0.0007	4.9	7.3
6	0.0096	10.9	28.5	37	0.0010	5.0	7.7
8	0.0008	6.3	9.6	38	0.0041	7.7	14.1
9	0.0130	14.4	25.1	39	0.0069	8.8	17.9
11	0.0146	9.9	23.4	40	0.0108	11.1	26.8
12	0.0106	10.6	21.9	41	0.0024	7.8	12.0
14	0.0046	6.6	11.5	42	0.0008	6.5	9.0
15	0.0000	5.8	9.5	43	0.0028	7.2	12.1
16	0.0199	16.6	24.2	44	0.0106	11.0	23.7
17	0.0259	21.0	27.4	45	0.0030	6.0	10.7
19	0.0048	6.4	11.4	46	0.0022	5.9	10.0
20	0.0083	9.7	21.4	47	0.0011	4.8	7.0
21	0.0121	11.7	26.9	48	0.0002	3.8	5.2
22	0.0026	8.2	14.9	49	0.0038	6.7	12.7
23	0.0049	7.8	14.4	53	0.0040	5.1	8.1
24	0.0102	9.7	20.1	54	0.0020	3.9	6.5
26	0.0000	4.3	6.3	56	0.0018	4.1	5.7
27	0.0094	8.8	17.9	57	0.0013	3.2	4.8
28	0.0056	6.2	11.2	58	0.0013	3.5	5.7
29	0.0064	6.2	11.7	59	0.0007	3.4	4.8
31	0.0012	4.8	7.6	60	0.0000	2.7	2.8
32	0.0009	4.2	5.7				
33	0.0053	7.9	14.6				

Table S5A. Relaxation rates as a function of CPMG effective field measured at 500 MHz. Sample conditions are: 15 °C, pH 6.0, 200 μM aS, 260 μM CR. Data used for determination of the parameters of aS/CR binding, and for generating Figure 5, main text.

Residue	R <sub>2</sub> (80 Hz)	R <sub>2</sub> (160 Hz)	R <sub>2</sub> (240 Hz)	R <sub>2</sub> (400 Hz)	R <sub>2</sub> (640 Hz)	R <sub>2</sub> (960 Hz)
3	6.5	6.1	6.0	5.3	4.5	4.2
4	8.6	8.2	8.1	7.0	6.0	5.5
6	10.9	10.8	9.0	8.9	7.2	6.8
8	6.3	6.2	6.2	5.8	5.2	5.1
9	14.4	12.6	11.9	10.1	8.2	7.5
11	9.9	9.2	8.2	7.1	6.1	4.4
12	10.6	9.4	9.0	7.0	6.5	4.6
14	6.6	5.8	5.6	5.0	4.4	4.0
15	5.8	5.6	5.3	4.7	4.3	4.1
16	16.6	13.1	12.2	9.7	7.5	5.4
17	21.0	19.0	19.2	15.6	11.0	8.9
19	6.4	5.7	5.3	4.8	4.1	3.6
20	9.7	8.7	7.7	6.4	5.3	4.9
21	11.7	9.0	8.8	7.6	6.1	5.2
22	8.2	7.8	7.1	6.5	5.9	5.3
23	7.8	6.9	6.5	5.5	5.1	4.9
24	9.7	9.2	8.2	7.1	5.8	5.2
26	4.3	4.1	3.9	3.6	3.5	3.2
27	8.8	8.0	7.5	6.3	4.9	4.0
28	6.2	5.4	5.1	4.3	3.9	3.5
29	6.2	5.8	5.0	4.2	3.8	3.7
31	4.8	4.2	4.4	3.9	3.7	3.5
32	4.2	4.0	3.8	3.7	3.4	3.4
33	7.9	7.4	6.8	5.9	5.6	4.7
35	7.4	7.0	6.5	5.8	5.0	4.6
36	4.9	4.4	4.3	3.9	3.7	3.5
37	5.0	4.8	4.5	4.2	4.0	3.8
38	7.7	7.4	6.1	5.3	4.7	4.2
39	8.8	8.5	7.8	7.0	6.1	5.4
40	11.1	9.8	9.1	8.0	6.6	5.6

Table S5A (continued)

Residue	R <sub>2</sub> (80 Hz)	R <sub>2</sub> (160 Hz)	R <sub>2</sub> (240 Hz)	R <sub>2</sub> (400 Hz)	R <sub>2</sub> (640 Hz)	R <sub>2</sub> (960 Hz)
41	7.8	6.9	7.0	6.3	5.5	4.9
42	6.5	6.3	6.0	5.7	5.5	5.3
43	7.2	6.8	6.8	6.1	5.8	5.5
44	11.0	10.2	9.7	8.6	7.2	6.1
45	6.0	5.7	5.7	5.1	4.6	4.5
46	5.9	5.6	5.4	4.9	4.4	4.1
47	4.8	4.2	4.0	3.8	3.5	3.7
48	3.8	3.7	3.6	3.4	3.3	3.1
49	6.7	5.9	5.3	4.7	4.1	3.7
53	5.1	4.7	4.6	3.9	3.6	3.3
54	3.9	3.7	3.6	3.4	3.2	3.0
56	4.1	3.7	3.7	3.2	2.9	2.6
57	3.2	3.1	3.1	2.8	2.6	2.5
58	3.5	3.3	3.2	3.1	2.8	2.6
59	3.4	3.1	2.9	2.8	2.6	2.5
60	2.7	2.7	2.6	2.6	2.4	2.3

Table S5B. Relaxation rates as a function of CPMG effective field measured at 900 MHz. Sample conditions are: 15 °C, pH 6.0, 200 μM aS, 260 μM CR. Data used for determination of the parameters of aS/CR binding, and for generating Figure 5, main text.

Residue	R <sub>2</sub> (80 Hz)	R <sub>2</sub> (160 Hz)	R <sub>2</sub> (240 Hz)	R <sub>2</sub> (400 Hz)	R <sub>2</sub> (640 Hz)	R <sub>2</sub> (960 Hz)
3	10.7	10.5	9.5	8.8	7.2	6.1
4	16.1	15.0	14.4	12.2	11.0	9.1
6	28.5	22.6	18.4	16.7	13.5	12.2
8	9.6	9.5	9.4	7.0	7.5	6.6
9	25.1	30.9	22.8	21.9	14.1	9.9
11	23.4	16.8	17.4	14.4	11.0	10.7
12	21.9	23.8	16.9	15.4	13.8	8.9
14	11.5	10.6	9.9	8.1	7.1	5.7
15	9.5	8.3	8.1	7.0	6.3	5.2
16	24.2	23.8	21.0	19.2	15.2	13.3
17	27.4	27.3	29.1	24.2	19.4	17.1
19	11.4	9.5	9.5	7.8	5.1	4.7
20	21.4	18.7	17.7	13.1	10.3	6.2
21	26.9	21.0	16.4	20.2	12.3	8.3
22	14.9	14.6	12.3	11.2	9.3	7.9
23	14.4	11.4	11.0	9.3	7.2	5.7
24	20.1	17.8	18.6	13.6	10.1	9.7
26	6.3	6.1	5.5	5.2	4.3	3.9
27	17.9	17.0	14.3	11.7	10.5	7.1
28	11.2	10.3	8.9	7.3	6.0	5.0
29	11.7	10.4	7.8	6.9	7.0	5.2
31	7.6	6.7	6.8	5.8	4.9	4.6
32	5.7	5.4	4.9	4.7	4.1	3.6
33	14.6	15.0	13.1	12.1	10.1	8.3
35	14.0	13.4	12.2	10.8	8.5	7.3
36	7.3	7.4	6.8	5.7	5.5	5.1
37	7.7	7.1	6.3	6.3	5.0	4.4
38	14.1	13.5	13.5	11.1	9.9	8.6
39	17.9	16.7	15.8	13.9	12.3	10.5
40	26.8	21.9	19.1	15.6	14.2	10.1

Table S5B (continued)

Residue	R <sub>2</sub> (80 Hz)	R <sub>2</sub> (160 Hz)	R <sub>2</sub> (240 Hz)	R <sub>2</sub> (400 Hz)	R <sub>2</sub> (640 Hz)	R <sub>2</sub> (960 Hz)
41	12.0	11.5	10.8	9.2	7.9	6.3
42	9.0	8.6	8.6	7.9	6.9	6.8
43	12.1	11.4	10.9	8.7	7.6	7.5
44	23.7	23.3	19.5	16.7	15.0	8.9
45	10.7	9.5	8.8	7.5	6.7	6.5
46	10.0	9.9	9.5	8.3	7.1	6.6
47	7.0	7.3	6.8	5.7	5.0	4.8
48	5.2	4.7	4.6	4.3	3.9	2.9
49	12.7	12.6	10.9	9.7	8.2	7.2
53	8.1	8.4	7.8	6.7	5.7	4.8
54	6.5	6.0	5.7	5.2	4.5	4.0
56	5.7	6.2	5.8	4.6	4.0	3.3
57	4.8	4.5	4.2	3.6	3.3	2.8
58	5.7	5.0	4.5	4.2	3.3	3.2
59	4.8	4.5	4.4	4.1	3.7	3.3
60	2.8	2.3	2.8	2.4	2.2	2.7

Table S6A. Intraresidue  $d_{\alpha N}(i,i)$  NOE build-up rate ( $s^{-1}$ ) and the ratio  $d_{\alpha N}(i,i)/d_{\alpha N}(i-1,i)$  for free aS, as measured in a 600 MHz 3D HNH NOESY-HMQC experiment (200  $\mu M$  aS). Values for Gly residues only (underscored) were corrected by dividing by 2. Data used for generating Figure 6, main text

Residue	Rate, $s^{-1}$	Rate error	Ratio	Ratio error	Residue	Rate, $s^{-1}$	Rate error	Ratio	Ratio error
3	0.097	0.003	0.317	0.009	77	0.121	0.003	0.166	0.003
4	0.096	0.003	0.305	0.008	80	0.205	0.004	0.234	0.004
5	0.202	0.005	0.452	0.010	81	0.173	0.003	0.189	0.003
6	0.154	0.003	0.337	0.008	83	0.151	0.002	0.254	0.004
8	0.179	0.004	0.388	0.008	<u>84</u>	0.187	0.003	0.306	0.005
<u>14</u>	0.337	0.003	0.511	0.005	85	0.124	0.002	0.539	0.010
17	0.193	0.003	0.266	0.004	<u>86</u>	0.203	0.003	0.839	0.013
22	0.289	0.004	0.377	0.005	87	0.114	0.003	0.324	0.007
26	0.173	0.002	0.480	0.006	88	0.100	0.002	0.251	0.005
27	0.220	0.003	0.407	0.006	89	0.150	0.002	0.299	0.005
<u>31</u>	0.264	0.004	0.485	0.007	91	0.146	0.003	0.315	0.005
32	0.190	0.003	0.498	0.009	<u>93</u>	0.263	0.004	0.584	0.008
33	0.192	0.004	0.263	0.005	95	0.146	0.003	0.200	0.004
37	0.205	0.003	0.451	0.006	96	0.206	0.003	0.190	0.003
38	0.211	0.003	0.219	0.004	98	0.234	0.003	0.343	0.004
39	0.220	0.003	0.266	0.004	<u>101</u>	0.249	0.003	0.500	0.005
40	0.224	0.004	0.235	0.004	102	0.210	0.002	0.475	0.006
<u>41</u>	0.451	0.005	0.472	0.005	103	0.213	0.003	0.387	0.005
42	0.334	0.008	0.297	0.007	104	0.168	0.002	0.513	0.007
44	0.248	0.004	0.329	0.005	<u>106</u>	0.253	0.002	0.484	0.004
48	0.164	0.002	0.322	0.004	107	0.112	0.002	0.275	0.005
53	0.157	0.003	0.200	0.003	109	0.155	0.002	0.220	0.003
54	0.159	0.003	0.184	0.003	<u>111</u>	0.307	0.002	0.471	0.004
58	0.237	0.003	0.230	0.003	113	0.176	0.003	0.179	0.003
63	0.180	0.003	0.190	0.003	116	0.115	0.003	0.151	0.004
64	0.172	0.003	0.181	0.003	118	0.197	0.003	0.133	0.002
65	0.119	0.004	0.183	0.006	121	0.316	0.004	0.492	0.005
<u>67</u>	0.212	0.003	0.458	0.006	125	0.231	0.003	0.286	0.004
69	0.076	0.002	0.269	0.006	126	0.314	0.005	0.217	0.003
70	0.086	0.002	0.187	0.004	130	0.216	0.003	0.243	0.003
71	0.119	0.003	0.180	0.004	135	0.170	0.003	0.284	0.005
72	0.123	0.003	0.175	0.004	139	0.072	0.002	0.180	0.004
<u>73</u>	0.238	0.003	0.421	0.006	140	0.031	0.002	0.180	0.010
75	0.147	0.003	0.192	0.004					
76	0.086	0.003	0.120	0.004					

Table S6B. Intraresidue  $d_{\alpha N}(i,i)$  NOE build-up rate ( $s^{-1}$ ) and the ratio  $d_{\alpha N}(i,i)/d_{\alpha N}(i-1,i)$  for CR:aS of 1:1, as measured from a 600 MHz 3D HNH NOESY-HMQC spectrum (200  $\mu M$  aS, 200  $\mu M$  CR). Values for Gly residues only (underscored) were corrected by dividing by 2. Data used for generating Figure 6, main text.

Residue	Rate, $s^{-1}$	Rate error	Ratio	Ratio errors	Residue	Rate, $s^{-1}$	Rate error	Ratio	Ratio errors
3	0.494	0.023	0.419	0.020	81	0.172	0.005	0.181	0.005
4	0.277	0.015	0.381	0.021	83	0.157	0.004	0.234	0.006
5	0.697	0.034	0.582	0.029	<u>84</u>	0.195	0.005	0.310	0.007
8	0.655	0.039	0.564	0.034	85	0.133	0.004	0.539	0.015
17	0.461	0.031	0.473	0.032	<u>86</u>	0.221	0.005	0.782	0.016
22	0.651	0.018	0.526	0.015	87	0.118	0.004	0.333	0.010
26	0.365	0.009	0.559	0.014	88	0.129	0.004	0.285	0.008
27	0.464	0.015	0.593	0.019	89	0.184	0.004	0.356	0.008
<u>31</u>	0.587	0.016	0.579	0.015	91	0.169	0.004	0.315	0.008
32	0.413	0.015	0.576	0.020	<u>93</u>	0.275	0.005	0.636	0.012
33	0.370	0.015	0.322	0.013	95	0.200	0.005	0.256	0.006
37	0.472	0.012	0.575	0.014	96	0.243	0.006	0.192	0.005
38	0.522	0.018	0.274	0.009	98	0.233	0.004	0.324	0.006
39	0.548	0.023	0.344	0.014	<u>101</u>	0.280	0.004	0.547	0.008
40	0.522	0.022	0.297	0.012	102	0.181	0.004	0.472	0.009
<u>41</u>	0.858	0.032	0.532	0.020	103	0.198	0.004	0.384	0.008
42	0.692	0.019	0.474	0.013	104	0.182	0.004	0.554	0.012
44	0.526	0.022	0.419	0.018	<u>106</u>	0.274	0.004	0.531	0.008
48	0.444	0.013	0.467	0.013	107	0.117	0.004	0.277	0.009
53	0.349	0.009	0.281	0.007	109	0.173	0.004	0.219	0.006
54	0.306	0.009	0.246	0.007	<u>111</u>	0.293	0.004	0.418	0.005
58	0.312	0.008	0.267	0.007	113	0.176	0.005	0.204	0.005
63	0.199	0.005	0.216	0.006	116	0.131	0.005	0.170	0.006
64	0.223	0.006	0.203	0.005	118	0.197	0.005	0.131	0.004
65	0.156	0.005	0.223	0.008	121	0.313	0.005	0.484	0.008
<u>67</u>	0.243	0.005	0.477	0.009	125	0.213	0.005	0.271	0.006
69	0.116	0.003	0.324	0.009	126	0.193	0.005	0.196	0.005
70	0.115	0.004	0.222	0.007	130	0.200	0.004	0.227	0.005
71	0.140	0.005	0.181	0.006	135	0.200	0.005	0.298	0.007
72	0.167	0.004	0.216	0.006	139	0.074	0.003	0.177	0.007
<u>73</u>	0.260	0.005	0.457	0.009	140	0.039	0.003	0.228	0.018
75	0.169	0.005	0.205	0.006					
76	0.109	0.005	0.143	0.006					
77	0.175	0.005	0.185	0.005					
80	0.213	0.005	0.232	0.006					

Table S6C. Intraresidue  $d_{\alpha N}(i,i)$  NOE build-up rate ( $s^{-1}$ ) and the ratio  $d_{\alpha N}(i,i)/d_{\alpha N}(i-1,i)$  for CR:aS of 4:1, as measured from a 600 MHz 3D HNH NOESY-HMQC spectrum (200  $\mu M$  aS, 800  $\mu M$  CR). Values for Gly residues only (underscored) were corrected by dividing by 2. Data used for generating Figure 6, main text.

Residue	Rate, $s^{-1}$	Rate error	Ratio	Ratio error	Residue	Rate, $s^{-1}$	Rate error	Ratio	Ratio error
64	0.620	0.051	0.287	0.024	<u>111</u>	0.268	0.007	0.331	0.009
<u>67</u>	0.533	0.020	0.518	0.020	112	0.118	0.006	0.216	0.012
69	—	—	0.360	0.015	113	0.174	0.009	0.174	0.009
70	0.279	0.014	0.291	0.014	114	0.220	0.008	0.288	0.010
71	0.375	0.024	0.212	0.014	116	0.115	0.013	0.153	0.017
72	0.344	0.017	0.251	0.012	118	0.166	0.010	0.113	0.007
<u>73</u>	0.510	0.017	0.515	0.017	121	0.277	0.009	0.496	0.017
74	0.298	0.012	0.341	0.014	125	0.147	0.007	0.237	0.011
75	0.358	0.016	0.274	0.012	126	0.123	0.006	0.183	0.009
76	—	—	0.207	0.014	130	0.123	0.008	0.188	0.012
77	0.339	0.021	0.234	0.015	<u>132</u>	0.238	0.007	0.530	0.016
78	0.432	0.019	0.311	0.014	135	0.145	0.007	0.322	0.015
80	0.451	0.026	0.304	0.017	139	0.103	0.008	0.231	0.017
81	0.260	0.019	0.158	0.011	140	0.034	0.005	0.222	0.032
83	0.303	0.013	0.290	0.012					
<u>84</u>	0.433	0.017	0.395	0.016					
85	0.301	0.011	0.587	0.022					
<u>86</u>	0.406	0.015	0.695	0.026					
87	0.252	0.012	0.453	0.022					
88	0.263	0.014	0.408	0.022					
89	0.425	0.023	0.485	0.026					
91	0.434	0.031	0.539	0.039					
<u>93</u>	0.583	0.032	0.622	0.034					
95	0.450	0.042	0.352	0.033					
96	0.391	0.037	0.252	0.024					
98	0.394	0.015	0.418	0.016					
99	0.467	0.015	0.618	0.020					
<u>101</u>	0.329	0.011	0.463	0.015					
102	0.333	0.010	0.578	0.018					
103	0.275	0.010	0.371	0.014					
104	0.217	0.008	0.570	0.021					
<u>106</u>	0.222	0.007	0.383	0.011					
107	0.127	0.007	0.287	0.016					
109	0.164	0.007	0.191	0.009					

Table S6D. Change in the ratio  $d_{\alpha N}(i,i)/d_{\alpha N}(i-1,i)$  for CR:aS of 1:1 and 4:1 as compared to free aS. Measured from a 600 MHz 3D HNH NOESY-HMQC spectrum. Values for Gly residues are not shown. Data used for generating Figure 6C, main text.

Residue	$\Delta$ Ratio CR:aS=1:1	$\Delta$ Ratio CR:aS=1:1 error	$\Delta$ Ratio CR:aS=4:1	$\Delta$ Ratio CR:aS=4:1 error
3	0.102	0.029		
4	0.076	0.029		
5	0.131	0.039		
8	0.175	0.042		
17	0.208	0.036		
22	0.149	0.020		
26	0.080	0.020		
27	0.186	0.025		
32	0.078	0.029		
33	0.058	0.018		
37	0.124	0.020		
38	0.055	0.013		
39	0.077	0.018		
40	0.063	0.017		
42	0.177	0.020		
44	0.090	0.023		
48	0.145	0.018		
53	0.080	0.011		
54	0.063	0.010		
58	0.036	0.010		
63	0.027	0.009		
64	0.022	0.008	0.106	0.027
65	0.040	0.013	—	—
69	0.055	0.015	0.092	0.022
70	0.035	0.011	0.104	0.019
71	0.001	0.010	0.032	0.018
72	0.042	0.009	0.076	0.016
75	0.013	0.010	0.082	0.016
76	0.024	0.010	0.088	0.018
77	0.020	0.009	0.069	0.018
80	-0.001	0.010	0.070	0.022
81	-0.008	0.008	-0.031	0.015
83	-0.019	0.010	0.036	0.016

Table S6D (continued)

Residue	$\Delta$ Ratio CR:aS=1:1	$\Delta$ Ratio CR:aS=1:1 error	$\Delta$ Ratio CR:aS=4:1	$\Delta$ Ratio CR:aS=4:1 error
85	0.001	0.025	0.048	0.032
87	0.009	0.018	0.128	0.029
88	0.034	0.014	0.157	0.027
89	0.057	0.013	0.186	0.031
91	0.001	0.013	0.225	0.044
95	0.055	0.010	0.152	0.036
96	0.002	0.008	0.062	0.027
98	-0.019	0.010	0.075	0.020
102	-0.003	0.015	0.103	0.023
103	-0.003	0.013	-0.016	0.019
104	0.041	0.019	0.056	0.028
107	0.002	0.013	0.012	0.021
109	-0.001	0.009	-0.029	0.012
113	0.025	0.008	-0.005	0.012
116	0.019	0.010	0.002	0.021
118	-0.002	0.006	-0.020	0.009
121	-0.008	0.014	0.005	0.022
125	-0.015	0.010	-0.049	0.015
126	-0.021	0.008	-0.033	0.012
130	-0.016	0.008	-0.055	0.015
135	0.014	0.012	0.037	0.019
139	-0.003	0.012	0.051	0.021
140	0.048	0.028	0.042	0.042

Table S7A. Sequential amide-amide NOE cross peak intensities, normalized by the diagonal peak intensity, as measured in a 600 MHz 3D NNH NOESY-HMQC experiment (15 °C, pH 6.0, 200 μM aS; 200 μM CR; 250 ms NOE mixing time). Data used for generating Figure 7B, main text.

Residue	NOE	Residue	NOE	Residue	NOE	Residue	NOE
4	0.143	40	0.061	78	0.026	125	0.033
7	0.057	41	0.112	79	0.022	126	0.030
8	0.062	42	0.065	80	0.025	130	0.024
9	0.147	43	0.088	81	0.028	131	0.026
10	0.091	44	0.119	82	0.025	132	0.021
11	0.107	45	0.067	83	0.024	133	0.024
12	0.102	46	0.089	84	0.019	134	0.020
13	0.142	47	0.072	85	0.023	135	0.021
14	0.111	48	0.077	86	0.020	136	0.018
15	0.110	49	0.063	87	0.027	137	0.015
16	0.112	50	0.056	88	0.029		
17	0.100	51	0.047	89	0.034		
18	0.093	52	0.028	90	0.024		
19	0.123	53	0.052	92	0.033		
20	0.116	54	0.041	93	0.048		
21	0.121	55	0.057	94	0.042		
22	0.107	56	0.059	95	0.031		
23	0.103	57	0.046	96	0.030		
24	0.069	58	0.054	98	0.040		
25	0.061	59	0.061	99	0.032		
26	0.079	60	0.052	100	0.046		
27	0.089	61	0.056	101	0.035		
28	0.082	66	0.026	104	0.033		
29	0.090	67	0.037	106	0.025		
30	0.063	68	0.026	107	0.029		
31	0.063	69	0.025	110	0.025		
32	0.090	70	0.018	111	0.020		
33	0.073	71	0.021	112	0.025		
34	0.044	72	0.024	113	0.022		
35	0.054	73	0.032	114	0.022		
36	0.084	74	0.030	115	0.033		
37	0.092	75	0.031	119	0.029		
38	0.087	76	0.031	123	0.052		
39	0.103	77	0.025	124	0.036		

Table S7B.  $d_{NN}(i,i+2)$  amide-amide NOE cross peak intensities, normalized by the diagonal peak intensity, as measured in a 600 MHz 3D NNH NOESY-HMQC experiment ( $15\text{ }^{\circ}\text{C}$ , pH 6.0,  $200\text{ }\mu\text{M}$  aS;  $200\text{ }\mu\text{M}$  CR; 250 ms NOE mixing time). Data used for generating Figure 7C, main text.

Residue	NOE	Residue	NOE
6	0.042	46	0.017
8	0.038	47	0.018
9	0.039	48	0.017
10	0.030	49	0.012
11	0.026	50	0.016
12	0.029	51	0.009
13	0.033	52	0.015
14	0.029	53	0.007
15	0.023	54	0.007
16	0.032	55	0.008
17	0.032	56	0.010
18	0.035	57	0.004
19	0.027	58	0.009
20	0.035	59	0.009
21	0.036	60	0.012
22	0.028	61	0.010
23	0.026	62	0.007
24	0.023	67	0.005
25	0.020	68	0.006
26	0.012	69	0.005
27	0.020	74	0.006
29	0.021	83	0.004
30	0.018	87	0.004
31	0.020	88	0.003
32	0.017	89	0.004
33	0.015	91	0.004
34	0.022	92	0.005
35	0.014	93	0.006
36	0.014	94	0.008
37	0.020	95	0.004
38	0.017	96	0.003
39	0.019	99	0.003
40	0.016	101	0.004
41	0.016	103	0.004
42	0.015	106	0.004
43	0.016		

Table S7C.  $d_{NN}(i,i+3)$  amide-amide NOE cross peak intensities, normalized by the diagonal peak intensity, as measured in a 600 MHz 3D NNH NOESY-HMQC experiment ( $15\text{ }^{\circ}\text{C}$ , pH 6.0,  $200\text{ }\mu\text{M}$  aS;  $200\text{ }\mu\text{M}$  CR; 250 ms NOE mixing time). Data used for generating Figure 7C, main text

Residue	NOE
7	0.010
10	0.016
16	0.016
17	0.017
18	0.019
19	0.015
20	0.016
21	0.021
22	0.013
25	0.010
26	0.012
28	0.012
29	0.009
30	0.006
31	0.011
32	0.009
33	0.006
36	0.008
37	0.008
39	0.008
40	0.008
47	0.010
48	0.008
52	0.012
57	0.006
59	0.004
87	0.003
89	0.003
90	0.005
93	0.004
95	0.005

Table S8A. Changes in aS  $^{13}\text{C}^\alpha$  chemical shifts induced by Congo Red, as measured by a 3D CT-HNCA experiment on perdeuterated  $^{13}\text{C}/^{15}\text{N}$ -labeled aS (15 °C, pH 6.0, 200  $\mu\text{M}$  aS, 500 MHz) for an CR:aS ratio of 1:1. Data used for generating Fig. 8, main text..

Residue	Delta CA						
3	0.004	39	0.004	75	0.001	110	0.012
4	0.009	40	0.003	76	0.000	111	-0.006
5	0.011	41	0.002	77	-0.001	112	-0.008
6	0.014	42	0.011	78	0.001	113	-0.011
7	0.020	43	-0.003	79	-0.001	114	0.021
8	0.018	44	-0.004	80	-0.001	115	0.020
9	0.028	45	0.003	81	0.000	116	-0.004
10	0.023	46	0.012	82	-0.001	117	-0.002
11	0.015	47	0.007	84	0.001	118	-0.010
12	0.014	48	0.003	85	0.000	119	0.040
13	0.007	49	0.001	86	0.000	120	-0.016
14	0.009	51	0.005	87	0.001	121	0.017
15	0.026	52	0.003	88	0.000	122	-0.001
17	0.019	53	0.009	89	0.001	123	0.019
18	0.012	54	-0.006	90	0.001	124	-0.025
20	0.023	55	0.003	91	-0.002	125	-0.009
21	0.012	56	0.003	92	0.000	126	0.016
22	0.019	57	0.013	93	0.000	127	-0.005
23	0.013	58	-0.002	94	0.002	128	-0.017
24	0.020	59	0.003	95	0.000	129	-0.013
25	0.020	60	0.000	96	0.001	130	0.01
26	0.018	62	0.000	97	-0.001	131	0.018
27	0.016	63	0.002	98	0.010	132	-0.006
28	0.022	64	0.003	99	-0.004	133	-0.004
29	0.011	65	0.000	100	0.000	134	-0.014
30	-0.002	66	0.002	101	-0.001	135	0.028
31	0.005	67	0.001	102	-0.002	136	-0.019
32	0.000	68	0.002	103	-0.001	137	0.04
33	-0.004	69	0.002	104	0.015	138	-0.002
34	0.006	70	0.001	105	0.019	139	0.037
35	0.011	71	0.002	106	-0.003	140	0.011
36	0.002	72	-0.001	107	-0.002		
37	0.002	73	0.000	108	-0.005		
38	0.005	74	0.001	109	-0.005		

Table S8B. Changes in aS  $^{13}\text{C}^\alpha$  chemical shifts induced by Congo Red, as measured by a 3D CT-HNCA experiment on perdeuterated  $^{13}\text{C}/^{15}\text{N}$ -labeled aS (15 °C, pH 6.0, 200  $\mu\text{M}$  aS, 500 MHz) for an CR:aS ratio of 4:1. Data used for generating Figure 8, main text.

Residue	Delta CA	Residue	Delta CA	Residue	Delta CA
62	0.112	96	0.022	130	0
63	0.107	97	0.059	131	0.023
64	0.073	98	0.042	132	-0.017
65	0.036	99	-0.018	133	0
66	0.026	100	0.025	134	-0.034
67	0.017	101	0.010	135	0.039
68	0.025	102	0.001	136	-0.021
69	0.027	103	-0.010	137	0.051
70	0.027	104	-0.026	138	-0.007
71	0.028	105	-0.006	139	0.057
72	0.002	106	-0.024	140	0.018
73	0.022	107	0.001		
74	0.028	108	-0.023		
75	0.032	109	-0.017		
76	0.036	110	0.007		
77	0.049	111	-0.014		
78	0.027	112	-0.004		
79	0.039	113	-0.021		
80	0.015	114	0.008		
81	0.018	115	0.024		
82	0.002	116	-0.007		
83	0.016	117	0.002		
84	-0.001	118	-0.016		
85	0.020	120	-0.046		
86	0.019	121	0.004		
87	0.064	122	-0.015		
88	0.088	123	0.022		
89	0.090	124	-0.035		
91	0.032	125	0.001		
92	0.044	126	0.013		
93	0.024	127	0.001		
94	0.069	128	-0.025		
95	0.015	129	-0.025		

Table S9A. Water-LOGSY effect for 1:1 CR:aS. Experiments were performed on perdeuterated  $^{15}\text{N}$ -labeled aS at 5 °C (pH 6.0, 200  $\mu\text{M}$  aS, 500 MHz spectrometer with a room temperature probe). Experiments involved application of a 2 second presaturation pulse ( $\gamma B_1 = 13 \text{ Hz}$  vs 0 Hz) followed by a normal HSQC sequence, and were collected in an interleaved manner. Data used for generating Figure 9, main text.

Residue	LOGSY effect	absolute error	Residue	LOGSY effect	absolute error
3	0.639	0.017	41	0.802	0.021
4	0.664	0.017	42	0.831	0.026
6	0.741	0.031	43	0.877	0.029
8	0.691	0.025	44	0.819	0.022
9	0.781	0.034	45	0.796	0.019
11	0.800	0.027	46	0.826	0.015
12	0.745	0.024	47	0.899	0.013
13	0.789	0.019	48	0.802	0.013
14	0.807	0.020	49	0.846	0.018
15	0.779	0.017	50	1.004	0.033
16	0.753	0.017	51	0.973	0.037
17	0.775	0.021	52	0.810	0.012
18	0.804	0.021	53	0.883	0.013
19	0.798	0.018	54	0.865	0.013
20	0.818	0.020	55	0.871	0.017
21	0.815	0.025	56	0.929	0.014
22	0.779	0.019	57	0.904	0.012
23	0.864	0.022	58	0.912	0.014
24	0.864	0.019	59	0.959	0.015
25	0.875	0.022	61	0.960	0.012
26	0.801	0.014	62	0.915	0.011
27	0.845	0.016	63	0.958	0.011
28	0.852	0.015	64	0.951	0.013
29	0.816	0.013	65	1.028	0.015
30	0.868	0.012	66	0.982	0.010
31	0.877	0.017	67	0.989	0.011
32	0.864	0.015	68	1.001	0.010
33	0.825	0.019	69	1.003	0.010
35	0.830	0.015	70	0.955	0.008
36	0.824	0.013	71	0.967	0.009
37	0.759	0.014	72	0.960	0.010
38	0.747	0.014	73	1.012	0.012
39	0.729	0.016	74	0.946	0.009
40	0.746	0.016	75	0.981	0.011

Table S9A (continued)

Residue	LOGSY effect	absolute error	Residue	LOGSY effect	absolute error
76	0.980	0.011	113	0.979	0.010
77	0.978	0.009	114	1.007	0.010
78	0.955	0.010	115	0.996	0.012
79	1.007	0.011	118	0.998	0.012
80	1.005	0.012	119	0.992	0.013
81	0.985	0.012	121	1.027	0.015
82	0.998	0.011	122	0.992	0.015
83	0.997	0.010	123	0.975	0.014
84	1.004	0.011	124	0.979	0.014
85	1.008	0.011	125	0.991	0.013
86	1.011	0.012	126	1.003	0.014
87	0.973	0.011	129	0.984	0.013
89	0.982	0.011	130	0.985	0.012
90	0.990	0.010	131	0.985	0.012
91	0.988	0.011	132	0.959	0.011
92	0.970	0.011	133	1.006	0.011
93	0.977	0.012	135	0.990	0.011
94	0.967	0.010	136	0.987	0.011
95	0.964	0.010	137	0.995	0.010
96	0.984	0.011	139	0.981	0.009
98	1.004	0.012	140	1.000	0.008
99	1.021	0.012			
100	0.991	0.011			
101	0.999	0.011			
102	0.987	0.010			
103	0.998	0.012			
104	1.002	0.011			
105	1.004	0.011			
106	1.001	0.010			
107	0.996	0.010			
109	1.007	0.010			
110	0.986	0.011			
111	0.998	0.011			
112	0.998	0.010			

Table S9B. Water-LOGSY effect for 4:1 CR:aS. Experiments were performed on perdeuterated  $^{15}\text{N}$ -labeled aS at 5 °C (pH 6.0, 200  $\mu\text{M}$  aS, 500 MHz spectrometer with a room temperature probe). Experiments involved application of a 2 second presaturation pulse ( $\gamma B_1 = 13 \text{ Hz}$  vs 0 Hz) followed by a normal HSQC sequence. Data used for generating Figure 9, main text.

Residue	LOGSY effect	absolute error	Residue	LOGSY effect	absolute error
59	0.341	0.083	97	0.880	0.018
60	0.635	0.072	98	0.851	0.013
61	0.588	0.033	99	0.880	0.013
62	0.643	0.027	100	0.871	0.012
63	0.697	0.022	101	0.876	0.011
64	0.642	0.025	102	0.892	0.010
65	0.833	0.024	103	0.920	0.012
66	0.738	0.013	104	0.946	0.011
67	0.795	0.015	105	0.959	0.010
68	0.786	0.011	106	0.944	0.009
69	0.795	0.010	107	0.973	0.010
70	0.765	0.009	109	0.968	0.009
71	0.759	0.011	110	0.958	0.010
72	0.745	0.012	111	0.978	0.010
73	0.798	0.013	112	0.971	0.009
74	0.775	0.010	113	0.989	0.010
75	0.740	0.012	114	1.003	0.011
76	0.781	0.012	115	0.977	0.011
77	0.772	0.010	118	1.004	0.011
78	0.800	0.012	119	0.978	0.012
79	0.856	0.013	121	1.016	0.013
80	0.846	0.015	122	0.969	0.013
81	0.805	0.013	123	0.955	0.011
82	0.801	0.011	124	0.965	0.011
83	0.825	0.011	125	0.992	0.011
84	0.834	0.012	126	0.979	0.012
85	0.815	0.012	129	0.981	0.011
86	0.808	0.013	130	0.985	0.010
87	0.773	0.012	131	0.978	0.010
89	0.779	0.013	132	0.980	0.009
90	0.773	0.012	135	0.976	0.009
91	0.771	0.014	136	0.951	0.008
92	0.772	0.016	137	0.977	0.008
93	0.776	0.016	139	0.967	0.007
95	0.756	0.015	140	0.989	0.007
96	0.791	0.015			

Table S10A. HSQC intensity attenuation ( $I/I_0$ ) of aS caused by an equimolar presence of CR, at 50  $\mu\text{M}$ . Data used for generating Figure S2.

Residue	$I/I_0$	Residue	$I/I_0$	Residue	$I/I_0$	Residue	$I/I_0$
3	0.233	46	0.363	86	0.878	125	0.968
4	0.211	47	0.387	87	0.873	126	0.968
6	0.101	48	0.234	88	0.877	129	1.000
8	0.139	49	0.210	89	0.877	130	0.997
9	0.095	50	0.151	90	0.859	131	1.016
11	0.111	53	0.348	91	0.822	133	1.047
12	0.092	54	0.391	92	0.857	134	1.024
14	0.234	56	0.473	93	0.821	135	0.995
15	0.201	57	0.522	94	0.882	136	1.027
16	0.079	58	0.474	95	0.805	137	0.993
17	0.072	59	0.564	96	0.851	139	0.996
18	0.105	61	0.748	98	0.877	140	0.996
19	0.172	63	0.763	99	0.912		
20	0.145	64	0.746	100	0.896		
21	0.077	65	0.791	101	0.928		
22	0.211	66	0.849	102	0.937		
23	0.185	67	0.841	103	0.912		
26	0.396	68	0.882	104	0.931		
27	0.173	69	0.899	105	0.919		
28	0.304	70	0.900	106	0.951		
29	0.266	71	0.860	107	0.948		
31	0.323	72	0.861	109	0.967		
32	0.266	73	0.867	110	0.939		
33	0.213	75	0.871	111	0.968		
35	0.272	76	0.890	112	0.951		
37	0.322	77	0.903	113	0.981		
38	0.323	78	0.876	114	0.943		
39	0.171	79	0.907	115	0.945		
40	0.170	80	0.866	118	0.982		
41	0.143	81	0.879	119	0.977		
42	0.315	82	0.872	121	0.963		
43	0.198	83	0.908	122	0.970		
44	0.103	84	0.870	123	1.023		
45	0.172	85	0.881	124	0.978		

Table S10B. HSQC intensity attenuation ( $I/I_0$ ) of aS caused by an equimolar presence of CR, at 6  $\mu\text{M}$ . Data used for generating Figure S2.

Residue	$I/I_0$	Residue	$I/I_0$	Residue	$I/I_0$	Residue	$I/I_0$
3	0.293	46	0.357	86	0.852	125	0.888
4	0.262	47	0.420	87	0.848	126	0.929
6	0.170	48	0.288	88	0.844	129	0.953
8	0.211	49	0.279	89	0.770	130	0.956
9	0.172	50	0.208	90	0.746	131	0.971
11	0.135	53	0.292	91	0.673	132	1.029
12	0.164	54	0.299	92	0.752	133	0.986
14	0.284	56	0.339	93	0.736	134	0.924
15	0.288	57	0.370	94	0.750	135	1.000
16	0.154	58	0.333	95	0.667	136	0.964
17	0.151	59	0.386	96	0.689	137	1.009
18	0.161	61	0.482	98	0.836	139	0.979
19	0.243	63	0.610	99	0.874	140	0.983
20	0.210	64	0.567	100	0.890		
21	0.122	65	0.699	101	0.928		
22	0.257	66	0.735	102	0.886		
23	0.199	67	0.758	103	0.899		
26	0.428	68	0.827	104	0.906		
27	0.229	69	0.814	105	0.927		
28	0.257	70	0.855	106	0.954		
29	0.257	71	0.752	107	0.886		
31	0.324	72	0.803	109	0.927		
32	0.268	73	0.797	110	0.896		
33	0.204	75	0.811	111	0.920		
35	0.250	76	0.799	112	0.897		
37	0.335	77	0.801	113	0.920		
38	0.381	78	0.770	114	0.950		
39	0.261	79	0.759	115	0.913		
40	0.200	80	0.725	118	0.963		
41	0.207	81	0.803	119	0.947		
42	0.364	82	0.805	121	0.947		
43	0.232	83	0.874	122	0.896		
44	0.160	84	0.846	123	1.004		
45	0.194	85	0.866	124	0.919		

Table S10C. HSQC intensity attenuation ( $I/I_0$ ) of aS caused by an equimolar presence of CR, at 2  $\mu\text{M}$ . Data used for generating Figure S2.

Residue	$I/I_0$	Residue	$I/I_0$	Residue	$I/I_0$	Residue	$I/I_0$
3	0.459	44	0.314	82	0.769	121	0.925
4	0.462	45	0.425	83	0.766	122	0.868
6	0.357	46	0.520	84	0.724	123	0.957
7	0.421	47	0.525	85	0.805	124	0.985
8	0.475	48	0.514	86	0.835	125	0.823
9	0.371	49	0.514	87	0.804	126	0.934
11	0.381	50	0.454	88	0.810	129	0.951
12	0.466	52	0.456	89	0.647	130	0.930
13	0.384	53	0.403	90	0.612	131	0.937
14	0.473	54	0.472	91	0.614	132	0.904
15	0.568	56	0.482	92	0.739	133	0.977
16	0.459	57	0.456	93	0.704	134	0.894
17	0.401	58	0.503	94	0.770	135	0.924
18	0.444	59	0.528	95	0.601	136	0.990
19	0.476	61	0.537	96	0.657	137	1.009
20	0.418	63	0.538	98	0.737	139	0.982
21	0.433	64	0.572	99	0.779	140	0.985
22	0.478	65	0.599	100	0.866		
23	0.439	66	0.625	101	0.780		
26	0.615	67	0.674	102	0.830		
27	0.471	68	0.806	103	0.904		
28	0.476	69	0.797	104	0.876		
29	0.430	70	0.712	105	0.877		
31	0.473	71	0.624	106	0.878		
32	0.427	72	0.720	107	0.892		
33	0.365	73	0.823	109	0.919		
35	0.459	74	0.877	110	0.879		
37	0.506	75	0.751	111	0.914		
38	0.533	76	0.708	112	0.869		
39	0.457	77	0.752	113	0.863		
40	0.414	78	0.704	114	0.891		
41	0.508	79	0.657	115	0.914		
42	0.521	80	0.628	118	0.937		
43	0.428	81	0.746	119	0.903		

Table S11. Backbone  $^{15}\text{N}$  and  $^1\text{H}^{\text{N}}$  chemical shift changes relative to free aS induced by a 5-fold molar ratio of CR:aS. Data used for generating Figure S3.

Residue	Delta N	Delta H	Residue	Delta N	Delta H
61	-0.095	-0.022	98	0.007	-0.008
62	-0.080	-0.019	99	0.014	-0.004
63	-0.089	-0.011	100	0.024	-0.005
64	-0.089	-0.013	101	0.010	-0.001
65	-0.028	-0.011	102	0.008	-0.004
66	-0.041	-0.011	103	0.038	-0.003
67	-0.056	-0.011	104	0.054	0.000
68	-0.012	-0.007	105	0.073	0.003
69	-0.008	-0.002	106	0.007	0.001
70	-0.023	-0.007	107	0.032	0.009
71	-0.043	-0.008	109	0.031	0.003
72	-0.026	-0.005	110	0.062	0.003
73	-0.016	-0.007	111	0.031	0.002
74	0.010	-0.003	112	0.045	0.005
75	0.006	-0.003	113	0.074	0.003
76	-0.010	-0.004	114	0.078	0.002
77	-0.005	-0.005	115	0.077	0.002
78	-0.015	-0.006	118	0.052	0.005
79	-0.011	-0.005	119	0.072	0.003
80	-0.001	-0.007	121	0.084	0.001
81	0.008	-0.003	122	0.050	0.007
82	0.013	-0.004	123	0.084	0.009
83	0.018	-0.003	124	0.084	0.004
84	-0.010	-0.003	125	0.130	0.006
85	0.001	-0.002	129	0.071	0.006
86	0.003	-0.003	130	0.061	0.003
87	0.003	-0.002	131	0.096	0.007
88	0.025	-0.003	132	0.060	0.005
89	-0.022	-0.005	133	0.060	0.003
90	-0.033	-0.006	134	0.104	-0.005
91	-0.029	-0.010	135	0.054	-0.003
92	0.000	-0.005	136	0.014	-0.002
93	-0.018	-0.008	137	0.092	0.003
94	0.008	-0.008	139	0.044	0.002
95	-0.021	-0.014	140	0.041	0.000
96	-0.043	-0.013			
97	-0.032	-0.015			

Table S12. Relaxation rates measured for a sample with CR:aS of 4:1 at 80 Hz CPMG effective field at 500 MHz and 800 MHz, as well as squared  $^{15}\text{N}$  chemical shift changes relative to free aS. Data used for generating Figure S4.

Residue	$[\Delta\delta\text{N}]^2$ , ppm $^2$	R2, Hz 500 MHz	R2, Hz 800 MHz	Residue	$[\Delta\delta\text{N}]^2$ , ppm $^2$	R2, Hz 500 MHz	R2, Hz 800 MHz
61	0.0090	10.5	15.6	97	0.0010	5.2	6.9
62	0.0064	9.6	12.7	98	0.0000	4.1	5.3
63	0.0079	9.4	12.9	99	0.0002	4.0	3.8
64	0.0079	9.9	14.7	100	0.0006	3.5	4.8
65	0.0008	5.8	6.8	101	0.0001	3.6	4.2
66	0.0017	5.3	6.2	102	0.0001	2.9	3.5
67	0.0031	5.8	6.4	103	0.0014	3.4	3.3
68	0.0001	4.7	4.6	104	0.0029	2.6	3.6
69	0.0001	3.8	4.1	105	0.0053	2.6	3.3
70	0.0005	4.5	5.4	106	0.0000	2.9	3.8
71	0.0018	5.1	7.0	107	0.0010	2.4	3.3
72	0.0007	5.4	6.5	109	0.0010	2.7	3.3
73	0.0003	5.2	5.4	110	0.0038	2.7	3.8
74	0.0001	4.3	4.7	111	0.0010	2.9	3.7
75	0.0000	5.4	6.4	112	0.0020	2.9	3.8
76	0.0001	5.1	5.6	113	0.0055	3.4	3.9
77	0.0000	5.0	5.9	114	0.0061	3.0	3.5
78	0.0002	5.1	6.4	115	0.0059	2.8	4.1
79	0.0001	4.9	5.5	118	0.0027	3.2	3.8
80	0.0000	5.1	5.9	119	0.0052	3.4	4.1
81	0.0001	4.8	6.2	121	0.0071	3.2	4.5
82	0.0002	4.4	5.1	122	0.0025	2.9	4.1
83	0.0003	4.2	5.6	123	0.0071	2.9	4.0
84	0.0001	4.3	5.0	124	0.0071	2.7	3.8
85	0.0000	3.7	3.9	125	0.0169	3.0	4.5
86	0.0000	5.0	5.7	129	0.0050	2.5	3.5
87	0.0000	4.6	5.4	130	0.0037	2.4	3.4
88	0.0006	4.8	5.5	131	0.0092	2.4	3.5
89	0.0005	5.9	8.3	132	0.0036	2.7	3.8
90	0.0011	5.4	7.8	133	0.0036	2.6	3.6
91	0.0008	5.3	7.2	134	0.0108	2.6	3.6
92	0.0001	6.5	8.1	135	0.0029	2.3	3.1
93	0.0003	5.5	6.4	136	0.0002	2.5	3.6
94	0.0001	5.0	5.5	137	0.0085	2.2	3.3
95	0.0004	6.7	10.4	139	0.0019	2.1	3.2
96	0.0018	6.0	7.9	140	0.0017	3.0	3.6

Table S13. Correlation of change in  $^{13}\text{C}^\alpha(i)$  chemical shift or residue i with the change in intra- to inter-residue  $^1\text{H}^\alpha\text{-}^1\text{H}^N$  NOE ratio of residue i+1  $d_{\alpha\text{N}}(i+1,i+1)/d_{\alpha\text{N}}(i,i+1)$ . Data are shown where available for the first 50 residues of aS. Data points that had a Gly as residue i or i+1 are not included. Comparison is between free aS and 1:1 CR:aS samples. Data used for generating Figure S7.

Residue	Ratio change	CA CS change
2	0.102	0.006
3	0.076	0.004
4	0.131	0.009
21	0.149	0.012
26	0.186	0.018
32	0.058	0.000
37	0.055	0.002
38	0.077	0.005
39	0.063	0.004
43	0.090	-0.003